



Open Archive Toulouse Archive Ouverte (OATAO)

OATAO is an open access repository that collects the work of Toulouse researchers and makes it freely available over the web where possible.

This is an author-deposited version published in: <http://oatao.univ-toulouse.fr/>
Eprints ID : 2547

To link to this article :

URL : <http://dx.doi.org/10.1103/PhysRevLett.97.127401>

To cite this version : Andrade, L.H.F and Laraoui, A. and Vomir, M. and Muller, D. and Stoquert, J.-P and Estournès, Claude and Beaurepaire, E. and Bigot, J.-Y (2006) [*Damped Precession of the Magnetization Vector of Superparamagnetic Nanoparticles Excited by Femtosecond Optical Pulses*](#). Physical Review Letters (PRL), vol. 97 (n° 12). pp.127401-1-127401-4. ISSN 0031-9007

Any correspondence concerning this service should be sent to the repository administrator: staff-oatao@inp-toulouse.fr

Damped Precession of the Magnetization Vector of Superparamagnetic Nanoparticles Excited by Femtosecond Optical Pulses

L. H. F. Andrade,¹ A. Laraoui,¹ M. Vomer,¹ D. Muller,² J.-P. Stoquert,² C. Estournès,³
E. Beaurepaire,¹ and J.-Y. Bigot¹

¹*Institut de Physique et Chimie des Matériaux de Strasbourg, (UMR 7504 CNRS-ULP), Strasbourg 67034, France*

²*Laboratoire PHASE (UPR 292 CNRS), Strasbourg 67034, France*

³*CIRIMAT (UMR 5085 CNRS-UPS-INP), Toulouse 31062, France*

The ultrafast magnetization and electron dynamics of superparamagnetic cobalt nanoparticles, embedded in a dielectric matrix, have been investigated using femtosecond optical pulses. Our experimental approach allows us to bypass the superparamagnetic thermal fluctuations and to observe the trajectory of the magnetization vector which exhibits a strongly damped precession motion. The magnetization precession is damped faster in the superparamagnetic particles than in cobalt films or when the particle size decreases, suggesting that the damping is enhanced at the metal dielectric interface. Our observations question the gyroscopic nature of the magnetization pathway when superparamagnetic fluctuations take place as we discuss in the context of Brown's model.

DOI: [10.1103/PhysRevLett.97.127401](https://doi.org/10.1103/PhysRevLett.97.127401)

PACS numbers: 78.47.+p, 75.50.Ss, 75.50.Tt, 78.20.Ls

Superparamagnetism consists in fluctuations of the magnetization in small ferromagnetic particles, resulting in a zero magnetization when it is averaged over a time scale larger than the typical time τ of these fluctuations. It occurs when the size of the magnetic particles is small enough so that the anisotropy energy becomes comparable to the thermal energy [1]. The fluctuation time τ generally varies over a very broad time scale, depending on the size of the particles. Superparamagnetism is relevant in several research fields like geophysics [2] and biophysics [3], as well as in the technology of high density information processing [4]. According to Néel's model, the fluctuations occur at a rate $1/\tau = 1/\tau_0 \exp(-KV/k_B T)$, where K , V , and T are, respectively, the anisotropy constant, the volume, and the temperature of the particle. Many studies have focused on the statistical aspect of the superparamagnetic fluctuations. The validity of this model of thermal activation over a single energy barrier has been demonstrated for a single ferromagnetic particle [5]. In contrast, little is known on the deterministic trajectory of the magnetization vector which is thought to undertake a gyroscopic motion while the fluctuations occur between the two opposite directions of the magnetization defined by the minima of the total free energy. This is supported by the seminal theoretical works of Néel [2] and Brown [6] who modeled the superparamagnetic fluctuations using two different approaches. Both models include a gyroscopic part either via random torques acting on the magnetization [2] or via the Landau-Lifschitz-Gilbert (LLG) equation in the presence of a fluctuating magnetic field [6]. This gyroscopic behavior shows up formally in the expression of the prefactor $1/\tau_0$ which, however, is not a well-known parameter (typical published values of τ_0 are dispersed in the range 10^{-8} – 10^{-12} s, depending on the material or experimental conditions). To our knowledge, there is so far no

real time study of the coherent dynamical regime associated with the gyroscopic motion of the magnetization in superparamagnetic systems. Several studies have been performed in the spectral domain [7], using Mössbauer spectroscopy, ferromagnetic resonance or neutron scattering [8].

In this Letter we focus on the coherent magnetization dynamics of superparamagnetic cobalt nanoparticles, independently of their thermal fluctuations. Our goal is to provide a method which allows us to determine the pertinent parameters associated with the coherent motion, i.e., the frequency ν and the damping time η of the magnetization precession, and to observe the trajectory of the magnetization for particles of different sizes. From the measured trajectory we deduce that the magnetization reversal cannot be a precessional one during the superparamagnetic fluctuations. To separate the coherent motion of the magnetization from its statistical fluctuations over the anisotropy energy barrier KV is an experimental challenge. It requires two important conditions. First, the temporal resolution of the experiment has to be much better than the characteristic times investigated (typically a few picoseconds). For this reason, the time resolved magneto-optical techniques using femtosecond pulses are well suited [9]. Second, an initial state has to be defined which is not sensitive to the randomness of the magnetization direction both in time (temporal fluctuations) but also from the point of view of a statistical averaging over a large number of independent particles (spatial fluctuations). In that case where a large number of particles is under interest it requires to bypass the thermal fluctuations by applying an external magnetic field which initially aligns the magnetization in a given direction. Naturally, the system under study must return to the initial state when a temporal averaging is necessary as it is the case with a repetitive

laser source. In our case we apply a static magnetic field H which can be varied between ± 4 kOe. Several experimental techniques have been developed during the past ten years to observe the ultrafast magnetization dynamics [10–17]. In the present work we adopted a configuration which allows us to probe the variation of the amplitude as well as the direction of the magnetization vector M and therefore to retrieve its trajectory in real time from a few femtoseconds up to 1 ns as detailed in Ref. [18]. In what follows, the quantities of interest are the static polar (Pol) and longitudinal (Long) magneto-optical signals, as well as their relative differential variation as a function of the pump-probe delay ($\Delta\text{Pol}(t)/\text{Pol}$ and $\Delta\text{Long}(t)/\text{Long}$) (relative difference between the signals with and without the presence of the pump pulse). They are obtained from a combination of Kerr measurements for the complementary angles θ , $-\theta$, and $\pi - \theta$ between the external magnetic field and the normal to the sample. In addition to the magnetization dynamics, information on the heating of the electrons and their relaxation to the lattice is obtained by monitoring the time dependent differential probe transmission $\Delta T(t)/T$ defined as the relative difference between the probe transmission measured with and without the pump pulse.

The cobalt nanoparticles are made by ion implantation of Co^+ in different matrices, at a temperature of 873 K, with different flux F , resulting in different particle diameters d as reported earlier [19,20]. Three different samples have been studied. Sample S1: matrix Al_2O_3 , $F = 10^{17} \text{ cm}^{-2}$, $d = 4 \pm 1 \text{ nm}$; sample S2: matrix Al_2O_3 , $F = 3 \times 10^{16} \text{ cm}^{-2}$, $d = 2.5 \pm 0.5 \text{ nm}$; and sample S3: matrix SiO_2 , $F = 10^{17} \text{ cm}^{-2}$, $d = 10 \pm 1 \text{ nm}$. Their implantation profile is determined by Rutherford backscattering spectrometry. For example, for the sample S1 it is a Gaussian peaking at 83 nm from the substrate surface and a width of 70 nm (maximum Co concentration 14%). At room temperature, the sample S3 is ferromagnetic, while S1 and S2 are superparamagnetic as seen in the magnetization curve $M(H)$ at room temperature represented in Fig. 1(a) for the sample S1. For the same sample, the zero field cooling (ZFC) and field cooling (FC) measurements are displayed

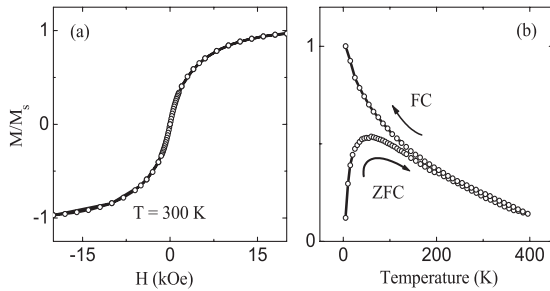


FIG. 1. Magnetization of 4 nm superparamagnetic cobalt particles in Al_2O_3 matrix at room temperature (a). Temperature variation of the magnetization for the field cooling (FC) and zero field cooling (ZFC) configurations (b).

in Fig. 1(b), showing that the blocking temperature T_B is $\sim 80 \text{ K}$.

Let us first focus on the diagonal part of the time resolved magneto-optical response which does not depend on the magnetization. The differential transmission of the sample S1 is represented in Fig. 2 for short [Fig. 2(a)] and long [Fig. 2(c)] temporal delays and for two different densities of laser pump energy ($I_1 = 5.1 \text{ mJ cm}^{-2}$ full line and $I_2 = 1.7 \text{ mJ cm}^{-2}$ open circles). The normalization factor for each curve is indicated. In Fig. 2(a) the cross correlation (normalized to -1) between the pump and probe beams is also displayed. From femtosecond optical studies of metal films and nanoparticles [21] it is known that the temporal variation of $\Delta T(t)/T$ contains several contributions associated with different relaxation mechanisms. The first one, which occurs within a few hundreds of femtoseconds, corresponds to the thermalization of the electrons excited high above the Fermi level by the pump pulse. This process is not instantaneous in metals due to the Pauli exclusion and it manifests by a delayed response of the differential transmission with respect to the pump excitation. The delayed response clearly shows up in Fig. 2(a) where the minimum of $\Delta T(t)/T$ occurs 350 fs after the cross correlation. The next important step in the dynamics is the equilibrium between the lattice and electron temperatures, a process which occurs via the electron-phonon interaction. The electron-lattice relaxation time τ_{el} increases when the density of pump energy increases because the electronic specific heat increases with the temperature. This is the case for the cobalt nanoparticles as seen in Fig. 2(a) where the time constants are, respectively, 1.6 ps and 0.8 ps for the excitation densities I_1 and I_2 . The variation of τ_{el} over one decade of pump intensity is displayed in Fig. 2(b). When the electrons and the lattice are in equilibrium, the thermal energy is transferred to the environment. This process can be decomposed into several steps depending on the nature of the environment. For a

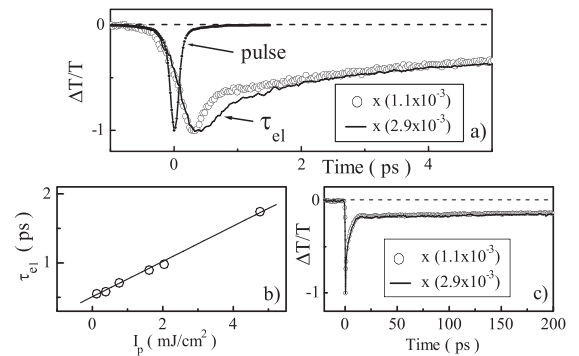


FIG. 2. Transmission dynamics of 4 nm superparamagnetic cobalt particles in Al_2O_3 . (a) short time behavior for two laser intensities $I_1 = 5.1 \text{ mJ cm}^{-2}$ (full line) and $I_2 = 1.7 \text{ mJ cm}^{-2}$ (open circles) together with the pump-probe cross correlation. (b) variation of the electron-lattice relaxation with the pump intensity. (c) long time behavior for I_1 and I_2 .

thin film of metallic particles with a diameter of a few nanometers isolated in a dielectric matrix (Al_2O_3 in the case of sample S1), the energy transfer from the particles to the dielectric is fast while the overall thermal diffusion outside the spatial region probed within the laser spot is much longer as seen in Fig. 2(c). The fast component is ~ 7 ps for the two densities of pump energy. This thermal relaxation process depends on the relative heat capacities between the metal and the dielectric as shown for silver particles embedded in different matrices [22]. The long-lived thermal diffusion occurs with a relaxation time of ~ 730 ps.

The dynamics of the magnetization is quite different. As shown in Fig. 3 for the sample S1, it displays an oscillatory behavior characteristic of a strongly damped motion of precession. It is clearly present in the projection of the magnetization trajectory displayed in the longitudinal/polar plane up to 1 ns [see Fig. 3(a)]. Figure 3(b) shows the corresponding time dependent differential polar ($\Delta\text{Pol}/\text{Pol}$) and longitudinal ($\Delta\text{Long}/\text{Long}$) components of the magnetization (displayed only up to 125 ps). The overall magnetization dynamics results from the ultrafast raise and subsequent decrease of the electron-spin temperature induced by the laser pump pulse, two processes which occur with time scales much faster than the motion of precession. In other words, the ultrafast change of temperature depicted in Fig. 2(a) acts as a δ function excitation of the magnetization which induces a change of both its modulus and orientation. The reorientation of the magnetization vector is due to a dynamical change of the effective field related to the time dependent anisotropy and exchange interactions as shown recently in the case of thin cobalt films [23]. The period and damping of the precession are respectively $1/\nu = 5 \times 10^{-11}$ s and $\eta = 9 \times 10^{-11}$ s, for an applied field $H = 2.8$ kOe. We find that ν varies from 14 to 25 GHz when H varies from 2.1 to 3.3 kOe. The correlation between the magnetization and the electron dynamics comes out by comparing Fig. 3(a) and Fig. 2(a). It is seen that the maximum of the demagnetization at 400 fs coincides with the thermalization of the electrons. Next, a partial remagnetization occurs within

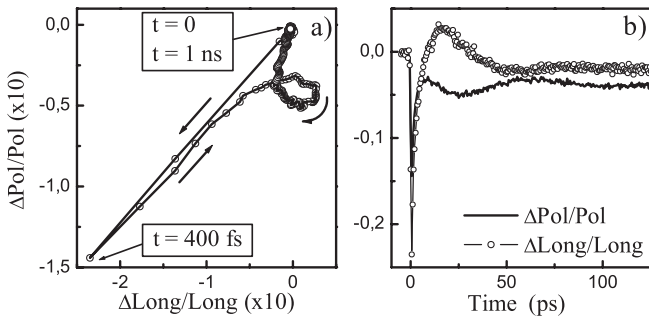


FIG. 3. Magnetization dynamics of 4 nm superparamagnetic cobalt particles in Al_2O_3 . (a) magnetization trajectory in the polar/longitudinal plane. (b) Dynamical polar and longitudinal Kerr signals.

~ 1 ps when the electrons cool down to the lattice via the electron-phonon interaction. Simultaneously, the orientation of the magnetization changes and starts precessing.

Let us examine how the precession damping η varies with the size of the particles. To do so, we have measured and compared η for the three samples S1, S2 (superparamagnetic with respectively ~ 4 and ~ 2.5 nm average diameter), and S3 (ferromagnetic ~ 10 nm average diameter) to the precession damping of a 16 nm thick cobalt epitaxial film grown on a Al_2O_3 substrate. In each case, we deduce the equivalent Gilbert damping α obtained from an approximate solution for the LLG equation valid for small damping [24]: $\frac{2}{M_S \eta \gamma_0}$ where $\gamma_0 = 2.4 \times 10^5 \text{ mA}^{-1} \text{ s}^{-1}$ is the gyromagnetic factor and M_S is the magnetization at saturation which is also measured for each sample. We get $\eta_{\text{film}} = 3 \times 10^{-10} \text{ s}$ (or $\alpha_{\text{film}} = 0.02$ using $M_{S,\text{film}} = 1.37 \times 10^6 \text{ A m}^{-1}$); $\eta_{10 \text{ nm}} = 1.2 \times 10^{-10} \text{ s}$ (or $\alpha_{10 \text{ nm}} = 0.43$ using $M_{S,10 \text{ nm}} = 1.6 \times 10^5 \text{ A m}^{-1}$); $\eta_{4 \text{ nm}} = 0.9 \times 10^{-10} \text{ s}$ (or $\alpha_{4 \text{ nm}} = 0.46$ using $M_{S,4 \text{ nm}} = 2 \times 10^5 \text{ A m}^{-1}$); $\eta_{2.5 \text{ nm}} = 0.6 \times 10^{-10} \text{ s}$ (or $\alpha_{2.5 \text{ nm}} = 3$ using $M_{S,2.5 \text{ nm}} = 4.5 \times 10^4 \text{ A m}^{-1}$). In that last case, the oscillation becomes hardly observable, the precession being critically damped and the above expression we use to estimate α is questionable. For each sample, we have checked that the precession period varies with the external static magnetic field H_0 . Also, we have observed that the contrast of the oscillations decrease as we decrease the amplitude of H_0 , showing that the effective field is dominated by H_0 . The damping is therefore much larger in the nanoparticles than in the bulk and, in addition, it consistently increases when the particle size decreases. The exact mechanisms of this enhanced damping observed in nanoparticles are still unknown but these results suggest that the metal dielectric interface plays an important role to damp the precession motion. It confirms previous studies of the magnetization damping in $\gamma\text{-Fe}_2\text{O}_3$ or cobalt nanoparticles. Using ac susceptibility and Mössbauer spectroscopy measurements, Dormann *et al.* [25] have reported a value of α close to unity for $\gamma\text{-Fe}_2\text{O}_3$ particles. Respaud *et al.* [26] have studied the ferromagnetic resonance of cobalt particles and reported values of α of 0.3 and 0.55 for particles containing respectively ~ 310 and ~ 150 cobalt atoms. They also attribute these large damping values to surface spin disorder. Another important conclusion which can be drawn from our measurements is that the damping of the precession is not affected by interparticle interactions for implantation densities up to 10^{17} cm^{-2} . Indeed, the cobalt particles of samples S1 and S2 are implanted in the same matrix, with a lower concentration for the smaller particles (sample S2) which nevertheless exhibit a larger Gilbert damping α . This result is not compatible with a strong interaction between particles which in the contrary should contribute to an increase of the damping when the concentration is larger [25]. It comforts the interpretation of a magnetic disorder at the particle-matrix interface as a source of damping for the magnetization precession.

Our study questions the possibility of the existence of a fully coherent pathway during the statistical superparamagnetic “jumps.” Even though our experiment is designed to prevent the fluctuations, for obvious reasons regarding the experimental methodology explained in the introduction, it turns out that the coherent part of the magnetization dynamics vanishes much faster than the average fluctuation time. This can also be deduced straightforwardly in the context of Brown’s description of superparamagnetism [27]. In his Langevin-like model, a transverse fluctuation is added in the LLG equation. The superparamagnetic fluctuations result both from the random torque exerted by this fluctuating field and the deterministic pathway of the magnetization under the action of the effective field. Following Brown, one obtains for the prefactor τ_0 :

$$\frac{1}{\tau_0} = \frac{2M_s\eta}{(M_s\eta)^2 + \gamma_0^{-2}} \sqrt{\frac{\mu_0 V M_s H_c^3}{2\pi k_B T}}, \quad H_c \equiv \frac{2K}{\mu_0 M_s}. \quad (1)$$

In this expression, two terms, which we name “coherent” and “incoherent” hereafter, contribute to $1/\tau_0$. The coherent term contains the parameters η and γ_0 of the gyroscopic motion and it is given by $\frac{2M_s\eta H_c}{(M_s\eta)^2 + \gamma_0^{-2}}$ while the incoherent term contains the ratio between the anisotropy energy barrier and the thermal energy and it is given by $\sqrt{\frac{\mu_0 V M_s H_c}{2\pi k_B T}}$. For the sample S1 one obtains at 300 K for $K = 0.57 \times 10^5 \text{ J m}^{-3}$: ($\tau_0 = 55 \times 10^{-12} \text{ s}$ with a coherent contribution of $21 \times 10^{-12} \text{ s}$ and an incoherent one of 2.6. Of course changes of K with particle size and/or embedding matrix can lead to different estimates of τ_0 . In conclusion, the present work shows that femtosecond magneto-optical techniques allow to investigate the coherent regime of the magnetization dynamics in superparamagnetic nanostructures. A comparison between different particles allows us to stress the drastic influence of the particles sizes on the damping of the precession. Within the simplified Brown’s model, all three temporal parameters τ_0 (prefactor in the magnetization relaxation), $1/\gamma_0 H_c$ (precession period), and η (damping) can have values of the same order of magnitude. In particular, for the smallest particles ($d < 4 \text{ nm}$) the precession motion is critically damped preventing the magnetization reversal to occur coherently. A complete gyroscopic pathway during the magnetization reversal is therefore unlikely to occur in such small superparamagnets.

We acknowledge a financial support from the European program “Dynamics.” L.H.F.A. would like to thank Centre National de la Recherche Scientifique for a grant.

[1] A. Aharoni, *Introduction to the Theory of Ferromagnetism* (Oxford University Press, New York, 2000), Chap. 5.

- [2] L. Néel, *Ann. Geophys.* **5**, 99 (1949).
- [3] D.P.E. Dickson and R.B. Franken, *Magnetic Properties of Fine Particles*, edited by J.L. Dormann, D. Fiorani (North Holland, Amsterdam, 1992), p. 393.
- [4] D. Weller, A. Moser, L. Folks, M.E. Best, W. Lee, M.F. Toney, M. Schwickert, J.-U. Thiele, and M.F. Doerner, *IEEE Trans. Magn.* **36**, 10 (2000).
- [5] W. Wernsdorfer, E.B. Orozco, K. Hasselbach, A. Benoit, B. Barbara, N. Demoncy, A. Loiseau, H. Pascard, and D. Mailly, *Phys. Rev. Lett.* **78**, 1791 (1997).
- [6] W.F. Brown, *J. Appl. Phys.* **30**, S130 (1959).
- [7] J.L. Dormann, D. Fiorani, and E. Tronc, *Adv. Chem. Phys.* **98**, 283 (1997).
- [8] M.F. Hansen, F. Bødker, S. Mørup, K. Lefmann, K.N. Clausen, and P.-A. Lindgård, *Phys. Rev. Lett.* **79**, 4910 (1997).
- [9] J.-Y. Bigot, C. R. Acad. Sci. Paris Ser. IV **2**, 1483 (2001).
- [10] E. Beaurepaire, J.-C. Merle, A. Daunois, and J.-Y. Bigot, *Phys. Rev. Lett.* **76**, 4250 (1996).
- [11] L. Guidoni, E. Beaurepaire, and J.-Y. Bigot, *Phys. Rev. Lett.* **89**, 017401 (2002).
- [12] A. Scholl, L. Baumgarten, R. Jacquemin, and W. Eberhardt, *Phys. Rev. Lett.* **79**, 5146 (1997).
- [13] M. Aeschlimann, M. Bauer, S. Pawlik, W. Weber, R. Burgermeister, D. Oberli, and H.C. Siegmann, *Phys. Rev. Lett.* **79**, 5158 (1997).
- [14] J. Hohlfeld, E. Matthias, R. Knorren, and K.H. Bennemann, *Phys. Rev. Lett.* **78**, 4861 (1997).
- [15] G. Ju, A. V. Nurmikko, R.F.C. Farrow, R.F. Marks, M.J. Carey, and B.A. Gurney, *Phys. Rev. Lett.* **82**, 3705 (1999).
- [16] M. van Kampen, C. Jozsa, J.T. Kohlhepp, P. LeClair, L. Lagae, W.J.M. de Jonge, and B. Koopmans, *Phys. Rev. Lett.* **88**, 227201 (2002).
- [17] A. V. Kimel, A. Kirilyuk, A. Tsvetkov, R. V. Pisarev, and Th. Rasing, *Nature (London)* **429**, 850 (2004).
- [18] M. Vomir, L.H.F. Andrade, L. Guidoni, E. Beaurepaire, and J.-Y. Bigot, *Phys. Rev. Lett.* **94**, 237601 (2005).
- [19] O. Cántora-González, D. Muller, C. Estournès, M. Richard-Plouet, R. Poinot, J.J. Grob, and J. Guille, *Nucl. Instrum. Methods Phys. Res., Sect. B* **178**, 144 (2001).
- [20] C. D’Orléans, J. Stoquert, C. Estournès, C. Cerruti, J.J. Grob, J.L. Guille, F. Haas, D. Muller, and M. Richard-Plouet, *Phys. Rev. B* **67**, 220101 (2003).
- [21] See, for example, Special issue on Electron Dynamics in Metals, edited by H. Petek and T.F. Heinz [*Chem. Phys.* **251**, 1 (2000)].
- [22] V. Halté, J.-Y. Bigot, B. Palpant, M. Broyer, B. Prével, and A. Pérez, *Appl. Phys. Lett.* **75**, 3799 (1999).
- [23] J.-Y. Bigot, M. Vomir, L.H.F. Andrade, and E. Beaurepaire, *Chem. Phys.* **318**, 137 (2005).
- [24] T.J. Silva, C.S. Lee, T.M. Crawford, and C.T. Rogers, *J. Appl. Phys.* **85**, 7849 (1999).
- [25] J.L. Dormann, F. D’Orazio, F. Lucari, E. Tronc, P. Prené, J.P. Jolivet, D. Fiorani, R. Cherkaoui, and M. Noguès, *Phys. Rev. B* **53**, 14 291 (1996).
- [26] M. Respaud, M. Goiran, J.M. Broto, F.H. Yang, T. Ould Ely, C. Amiens, and B. Chaudret, *Phys. Rev. B* **59**, R3934 (1999).
- [27] W.F. Brown, *Phys. Rev.* **130**, 1677 (1963).